Cytotoxic effects of molybdenum oxide nanoparticles and {Mo36} polyoxomolybdate nanoclusters to the green microalga Chlorella vulgaris

Hanifeh Akbarian Kalehjahi
University of Tabriz
Morteza Kosari-Nasab
University of Tabriz
Mojtaba Amini
University of Tabriz
Ali Movafeghi (movafeghi@tabrizu.ac.ir)
University of Tabriz https://orcid.org/0000-0002-4134-6986

Research Article

Keywords: Chlorella vulgaris, MoO3 nanoparticles, Polyoxomolybdate, Oxidative stress, Toxicity, Antioxidant enzymes

Posted Date: July 6th, 2022

DOI: https://doi.org/10.21203/rs.3.rs-1742905/v1

Abstract

In recent years, molybdenum-based nanomaterials have been widely used in different industrial sectors because of their multifunctional properties. Despite their extensive industrialization, there is a lack of needed information concerning their adverse influences on ecosystems and living organisms. In this study, molybdenum oxide nanoparticles (MoO_3 NPs) and {Mo_{36}} polyoxomolybdate nanoclusters ({Mo_{36}} NCs) were synthesized using hydrothermal methods and characterized using FT-IR, XRD, and SEM techniques. Subsequently, their toxic effects on the green microalgae *Chlorella vulgaris* were measured. Both nanomaterials (NMs) induced cytotoxicity by reducing the cell number and biomass of algae in a dose- and time-dependent manner. Scanning electron microscopy revealed shape modification and plasmolysis of the microalgal cells after exposure to nanomaterials. Flow cytometric analyses confirmed the reduction in cell viability in the samples exposed to 100 mg L^{-1} of MoO_3 NPs and {Mo_{36}} NCs for 4 days. According to the results, MoO_3 NPs had more drastic effects on the viability of *C. vulgaris* cells compared to {Mo_{36}} NCs. In addition, after exposure of algal cells to the high concentrations of nanomaterials, the content of photosynthetic pigments has decreased. Enhanced activities of antioxidative enzymes including superoxide dismutase (SOD), catalase (CAT), and ascorbate peroxidase (APX) concurrent with alteration of phenol and flavonoid contents as non-enzymatic antioxidants indicated the activation of cell defense systems in response to the oxidative stress induced by nanomaterials. Our findings conclusively established that MoO_3 NPs and {Mo_{36}} NCs cause life-threatening cytotoxicity in algal cells and induce oxidative stress.

Introduction

Over the last few decades, the production of nanomaterials (NMs) has remarkably increased due to the identification of their particular physical, chemical and biological properties. The widespread use of NMs in various industrial products has resulted in their unintended release into the biosphere (Giese et al., 2018). Thus, it is necessary to analyze their performance under different environmental conditions and their possible hazardous impacts on living organisms. In point of fact, serious concerns have been raised in the last few years regarding the evaluation and management of environmental risks of NMs (Malakar et al., 2021; Zhao et al., 2021). However, awareness of the potential threats of NMs to living organisms remains in its primary steps.

Molybdenum (Mo) is a widespread naturally occurring transition element in aquatic and terrestrial environments. This element is necessary for the physiology of living organisms, because it is involved in the function of enzymes catalyzing several essential biochemical reactions (Mendel and Bittner, 2006). In recent years, the industrial utilization of molybdenum-based NMs has intensified in comparison to corresponding bulk materials. Nanostructured molybdenum oxide nanoparticles (MoO_3 NPs) have broad-spectrum applications and were effectively used in super-capacitors, photo-catalysis, electro-catalysis and gas sensors (Cheng et al., 2009; Xue et al., 2021). MoO_3 NPs have also broadly used in the biomedical field owing to their antibacterial and antifungal activity (Shafaei et al., 2017; Alghamdi, 2020).

Likewise, polyoxomolybdate nanoclusters (NCs) have attracted attention because of their infinite architectures and excellent redox capabilities. Polyoxomolybdate NCs have been employed in the fields of catalysis, analytical chemistry, inorganic chemistry, material science, biological sciences and medicine (Amini et al., 2015; Jalilian et al., 2015; Stamate et al., 2020). The wide application of molybdenum-based NPs and NCs leads to their unsafe discharge into the environment. Thus, their fate and behavior in the ecosystems and their physiological and biochemical interactions with living organisms should be precisely evaluated (Forloni, 2012; Suhendra et al., 2020).

Microalgae are widely used as ideal organisms for assessing the toxicity of different pollutants owing to their abundant availability, fast growth rate, simple culture procedure and high sensitivity to environmental contamination (Cheng et al., 2016; Nazari et al., 2018). Importantly, microalgae are in the first line of the fight against environmental pollution (Monteiro et al., 2012). The green unicellular microalga *Chlorella vulgaris* (*C. vulgaris*) with a wide distribution range in seawater and freshwater is a well-known model biosystem for cell-based toxicological analysis (Movafeghi et al., 2019; Khoshnamvand et al., 2020). This phytoplankton species has been also recognized to have an outstanding potential for the elimination of various environmental contaminants (Kalhor et al., 2017; Asghari et al., 2020). Hence, in the current work, we examined a number of growth and developmental indices of *C. vulgaris* after exposure to molybdenum-based NMs. In addition, the impacts of molybdenum-incorporated NPs and NCs on cell viability as well as enzymatic and nonenzymatic cellular antioxidant defense systems were considered. The obtained results may throw new light on the safety risks of manufactured NMs and their impacts on biological systems.

Materials And Methods

Synthesis and characterization of MoO_3 NPs

MoO_3 NPs were synthesized according to a previously reported method (Amini et al., 2015). At first, 4 mmol of $Na_2MoO_4{\cdot}2H_2O$ was dissolved and stirred in 6M HCL to obtain $MoO_3.nH_2O$ particles. Afterwards, the gained solids were washed several times with water, dried at 50°C, and then calcined at 500°C for 3 h to obtain MoO_3 nanoparticles. Structure of the synthesized NPs was investigated by utilizing X-ray powder diffraction (XRD), Fourier-transform infrared spectroscopy (FT-IR) and scanning electron microscopy (SEM).

Synthesis and characterization of $\{Mo_{36}\}$ NCs

$\{Mo_{36}\}$ NCs were synthesized using the previously reported technique (Amini et al., 2015). Sodium molybdate (4.9 mmol) and hydroxylamine hydrochloride (1.11 mmol) were dissolved in 30 ml water. After adding 1 ml of 4 % HCL and adjusting the pH of the solution to 3, solution was reflexed for 20 h. The hot solution was filtrated and the red deposit was kept for crystallization. The structure of the synthesized $\{Mo_{36}\}$ NCs was defined using X-ray powder diffraction (XRD), energy dispersive X-Ray (EDX), and Fourier-transform infrared spectroscopy (FT-IR).

Culture condition for algal cells

The cells of *C. vulgaris* strain CCAP 211/11B were cultivated under aseptic condition in BG-11 medium with continuous shaking under cool white fluorescent light (illumination intensity: 5000 lux) at 25 °C. Cell counting was performed every 24 h using a hemocytometer and a light microscope (Olympus, Japan). The regression equation between cell number (y × mL) and OD_{680} (x) was attained as y = 138.98x + 4.5093 (R2 = 0.9932). Growth of the algal cells was also examined by changes in OD_{680} using a spectrophotometer (SPEKOL 1500, Jena, Germany). Treatments of the algal cells with MoO_3 NPs and $\{Mo_{36}\}$ NCs were conducted in the exponential growth phase on the 6^{th}-8^{th} day of culture. 100 ml Erlenmeyer flasks containing 50 ml of algal cell culture were exposed to both NMs with the final concentrations of 25, 50, 75, 100 mg L^{-1}. After 96 h of exposure in a light incubator, treated cells were collected by centrifugation at 5000 g for 10 min and kept at -80 °C until use for different assessments.

Measurement of growth parameters

Estimation of algal growth was daily performed by counting the cells and by measuring the optical density at 680 nm with a spectrophotometer. The exponential phase of *C. vulgaris* was explored and used for treatment of cells with different concentrations of MoO_3 NPs and $\{Mo_{36}\}$ NCs. An initial cell number of 30* was considered for all experiments. Fresh weight was determined after harvesting the cells by centrifugation at 5000 g for 10 min. Dry weight was measured after 48 h drying period of the cells at 40°C.

Scanning electron microscopy of cells

After exposure of algae to 100 mg L^{-1} of MoO_3 NPs and $\{Mo_{36}\}$ NCs for 96 h, the culture media were centrifuged at 5000 g for 10 min. The obtained cells were rinsed several times with medium, freeze-dried for 1 h and coated with gold, prior to be observed under SEM (MIRA3 FEG-SEM, Tescan, Czech Republic).

Flow cytometric analysis

Flow cytometric assays were carried out to check the viability of *C. vulgaris* cells treated with 100 mg L^{-1} of MoO_3 NPs and $\{Mo_{36}\}$ NCs for 96 h. Around 1.0×10^{6} cells were collected by centrifugation (5000 g, 10 min), washed with phosphate buffer solution (PBS, pH 7.4), and stained with 5 µl propidium iodide (PI) for 30 min in the dark. The fluorescence emission of the samples was acquired from ~10,000 events per cell sample in the BD FACSCalibur FL2 channel. The emitted chlorophyll fluorescence was gathered in the FL3 channel.

Measurement of photosynthetic pigments

Content of photosynthetic pigments including chlorophyll a, b, and carotenoids was assessed using methanolic extract of algae by a formerly reported standard procedure employing a double-beam UV-visible spectrophotometer (SPEKOL 1500, Jena, Germany) (Wellburn, 1994).

Assessment of total protein and antioxidant enzyme activities

The obtained algal cells by centrifugation were ground in liquid nitrogen prior to be homogenized in 2 ml of phosphate buffer (100 mM, pH 7) at 4 °C. The acquired homogenate was centrifuged at 10000 g for 10 min at 4° C. The supernatant was utilized for assessing the amount of total protein content (Bradford, 1976). The activity of catalase (CAT) was evaluated based on the method of Chance and Maehly (1955), where one µmol of reduced H_2O_2 per minute presented one unit of enzyme activity. Superoxide dismutase (SOD) activity was assessed by measuring the prevention of photoreduction of nitro blue tetrazolium (NBT) through algal extract. Once NBT is inhibited to be reduced by 50% through enzyme action, it indicates one unit of SOD activity (Winterbourn et al., 1976). The activity of ascorbate peroxidase (APX) was recognized by the oxidation of ascorbate with the algal extract. One unit of enzyme activity was considered as the amount required for oxidation of 1 µM ascorbic acid in one minute (Nakano and Asada, 1981).

Determining the content of phenols and flavonoids

The total phenol content was measured according to the Folin-Ciocalteu method (Meda et al., 2005). Concisely, 100 µL of the methanolic extract of cells was added to 2.5 mL of distilled water and 100 µL of Folin-Ciocalteu. Subsequently, 150 µL of sodium carbonate (20%) was added and kept at room temperature in a dark room for 30 minutes. Then, the absorbance of the mixture was determined at 760 nm. The total phenol amount was evaluated equivalent to a standard graph of gallic acid as milligram gallic acid per fresh weight of microalgae. Measurement of total flavonoid content was conducted using a modified aluminum chloride colorimetric procedure (Chang et al., 2002). An amount of 500 µL aluminum chloride (2%) was mixed with 500 µL of methanolic extract. After keeping the solution at 4°C for one hour in the dark, its absorbance was assessed at 415 nm. Total flavonoid content of the samples was considered as milligram quercetin equivalent per fresh weight of algal cells.

Statistical analysis

One-way analysis of variance (ANOVA) was directed with Duncan's multiple comparison tests by SPSS software. Tests were performed in triplets. The values were distinguished as significantly different when the probability was a smaller amount than 0.05.

Results And Discussion

Structural description of MoO_3 NPs

The as-prepared compound was initially characterized by X-ray diffraction (XRD). The XRD pattern of the MoO_3 powders is plotted in Fig. 1A, showing that peaks match well with the single phase of MoO_3 NPs monoclinic phase without other unidentified peaks of impurities. The peaks at 875cm^{-1} and 611 cm^{-1} at IR spectrum are related to symmetric and antisymmetric stretching modes of O–Mo–O bond respectively (Fig. 1B). To know the information about the surface of the material, the scanning electron microscopy

(SEM) image of particles was obtained (Fig. 1C). According to SEM image, MoO_3 particles are formed with diameters in the range of 70-100 nanometers.

Structural characterization of {Mo_{36}} NCs

Synthesized {Mo_{36}} was red in color and absolutely stable in front of air, moisture and light. Of note, particles were completely soluble in water, methanol, ethanol, acetonitrile, DMF and DMSO. According to previously reported X-ray diffraction analyses, the formula of the {Mo_{36}} compound was confirmed to $[Mo_{36}O_{110}(NO)_4(H_2O)_{14}]$ with a large cluster of {Mo_{36}} skeleton, which comprises two 18–molybdate {$Mo_{18}O_{55}$} subunits associated with each other by an inversion center (Fig. 2A). Energy dispersive X-Ray (EDX) analysis of the {Mo_{36}} NCs showed that the crystals consisted of molybdenum and oxygen (Fig. 2B). Furthermore, IR spectrum of {Mo_{36}} indicated a wide band that shows coordinated H_2O in 3415 cm^{-1}. The peaks at 865cm^{-1},614 cm^{-1} and 1626 cm^{-1} are related to Mo=O, Mo–O–Mo and NO bonds respectively (Fig. 2C).

The effect of MoO_3 NPs and {Mo_{36}} NCs on the growth of *C. vulgaris*

Evaluating the changes in cell number, fresh and dry weight of *C. vulgaris* during 4 days of experiments confirmed the concentration-dependent influence of Mo-based NPs and NCs on the growth of algal cells (Fig. 3). Intriguingly, in the first three days of experiments the cell number of algae has enhanced after exposure to low concentrations (25 and 50 mg L^{-1}) of MoO_3 NPs and {Mo_{36}} NCs compared to the control samples (Fig. 3A, B). On the other hand, higher concentrations of MoO_3 NPs and {Mo_{36}} NCs (75 and 100 mg L^{-1}) diminished the cell number from the first day of the treatment. Actually, after 4 days the inhibitory effects of the increasing concentrations of NPs and NCs on the cell number were more evident. Fresh and dry weights of treated cells were typically reduced by the rising concentration of MoO_3 NPs and {Mo_{36}} NCs (Fig. 3C- F). Based on the obtained results, treatment with 100 mg L^{-1} of NP and NC resulted in the highest inhibitory effects on fresh and dry weight of algal cells.

Stimulatory hormetic impacts of NMs on algae were described in some of the preceding studies. For instance, an increase in the growth rate of *Chlorella pyrenoidosa* after exposure to low amounts of Fe_3O_4 nanoparticles and a decrease with the increasing concentration of nanoparticles was reported (Wang et al., 2021). Another study showed that nanoparticles release elements after attachment to cell walls, and consequently enhance the algal growth (Lütz-Meindl and Lütz, 2006). Similarly, it was revealed that engineered nanoparticles could act as a stock producer to the organisms (Navarro et al., 2008). The stimulating effect of zinc and iron micronutrients at low concentrations and their toxic effect at higher doses were mentioned as the reason for this cellular response. Thus, simulative and toxic impacts of molybdenum based NPs and NCs on the growth of *C. vulgaris* respectively at low and high concentrations seems to be reasonable. Presumably, there is a concentration threshold for the applied NMs for each biosystem (Juárez-Maldonado et al., 2021). Below this precise value the biological responses of cells are positive. Once the concentration is exceeded the threshold value, the observed

effect, for example on growth criteria, become negative. The decline in cell number, fresh and dry weight of the algae after exposure to the increasing concentration of NPs and NCs was possibly because of their disrupting effect on the membrane integrity, the metabolic processes of cells and the activity of the enzymatic systems resulting in preventing the cell growth (Bhuvaneshwari et al. 2015; Movafeghi et al. 2018; Wang et al. 2019). Manufactured nanomaterials could also cause the generation of reactive oxygen species (ROS), which may lead to oxidative damages to intracellular structures (Movafeghi et al., 2019).

Morphology of the cells after exposure to MoO_3 NPs and $\{Mo_{36}\}$ NCs

Study of cells by SEM disclosed remarkable shrinkage of the treated cells with the both types of NMs (Fig. 4). In comparison with intact and turgescent control cells (Fig. 4A, B), the cells exposed to 100 mg L^{-1} of MoO_3 NPs (Fig. 4C, D) and $\{Mo_{36}\}$ NCs (Fig. 4E, F) demonstrated evident morphological changes. The cells exposed to MoO_3 NPs were massively plasmolysed and shrunk with visible damages on their surfaces. In comparison, exposure of cells to $\{Mo_{36}\}$ NCs caused shape modification to a lesser extent. Noticeably, $\{Mo_{36}\}$ NCs affect the cell morphology less than MoO_3 NPs. Comparable effects of NMs on cell surface deformations of microalgae were previously reported (Fazelian et al., 2019; Movafeghi et al., 2019). $\{Mo_{36}\}$ NCs are completely soluble in aqueous solutions, and thus their cytopathic effects on microalgae may be explained by their solubility features and also by the release of molybdenum ions into the culture medium (Amini et al., 2015). By contrast, MoO_3 NPs are not soluble in aqueous media and their adsorption on the surface of cells beside the release of ions feasibly led to the higher toxicity impact. Since the surface of algal cells could be occupied by nanoparticle, the direct physical contacts may result in reducing the accessibility of light and nutrients, and cause cell deformation (Pereira et al., 2014; Saxena et al., 2021).

Cell viability analysis by flow cytometry

Evaluating the cell viability after exposure the cells of *C. vulgaris* to 100 mg L^{-1} of MoO_3 NPs and $\{Mo_{36}\}$ NCs were conducted using flow cytometry. The red fluorescent nucleic acid dye PI can pass into the damaged dead cells, bind to double-stranded DNA molecules and emit red fluorescence (Asghari et al., 2020). Thus, PI could be used to distinguish dead fluorescent cells from live unstained cells (Suman et al., 2015). In flow cytometry diagrams, the upper left and right quadrants reveal the percentage of dead cells, the both lower quadrants indicate the proportion of viable cells and the lower right quadrant represents chlorophyll fluorescence (Fig. 5). We observed almost 92% of cell viability of the control sample after 96 h of culture and all the cells displayed chlorophyll fluorescence (Fig. 5A). Nevertheless, the amount of viable cells in the culture media exposed to 100 mg L^{-1} of $\{Mo_{36}\}$ NCs has decreased to 87.6% and just 5% of the viable cells didn't show chlorophyll fluorescence (Fig. 5B). The drastic effect was detected after exposure of cells to MoO_3 NPs. The amount of viable cells has decreased to be 56.94% after 96 h of treatment and 5.21% of viable cells did not display chlorophyll fluorescent (Fig. 5 C).

These outcomes are in agreement with the findings of scanning electron microscopy examinations presenting the higher toxic influences of MoO_3 NPs compared to $\{Mo_{36}\}$ NCs on the studied algal cells.

The influence of MoO_3 NPs and $\{Mo_{36}\}$ NCs on the content of photosynthetic pigments

After a 4-day-exposure, the impact of the applied concentrations of NPs and NCs on the content of photosynthetic pigments was detected as a hormesis phenomenon. Exposure to 25 and 50 mg L^{-1} of MoO_3 NPs increased the amount of chlorophyll a and b in algal cells, although the higher concentrations of NPs could significantly lower the amounts of chlorophylls (Fig. 6A, C). By contrast, the chlorophyll a and b contents have risen after treatment with 25, 50, and 75 mg L^{-1} of $\{Mo_{36}\}$ NCs and then went down at the concentration of 100 mg L^{-1} (Fig. 6B, D). Likewise, amount of carotenoids has elevated after exposure to low concentrations of NPs and NCs, and thereafter has decreased at high levels of nanomaterials (Fig. 6E, F). These findings are in line with some former experiments on *Chlorella vulgaris* indicating the decline of photosynthetic pigments with the increasing concentration of NMs (Xiaoxiao et al., 2012; Cheng et al., 2016). Additionally, a subsequent decrease of pigment content concurrent with the rising concentration of nanoparticles was reported (Metzler et al., 2012; Taghizadeh et al., 2020). Metal ion release from soluble metal oxide nanomaterials in aqueous solutions is one of main reasons for their repressive effect on photosynthetic system (Wang et al., 2016). The bioavailability of some nutrients can be inhibited by NMs that can also cause toxic effects (Ji et al., 2011; Metzler et al., 2012). Indeed, the content of photosynthetic pigments could be regarded as a significant biomarker of photosynthetic potential in aquatic plants and algae (Movafeghi et al., 2018; 2019). Thus, any decline in their content by changing the experimental factors designates the reduction in photosynthetic competence which may result in growth weakening as was recognizable in our experiments. The descending content of photosynthetic pigments is also regarded as one of the oxidative stress indicators. Therefore, the reduction of chlorophyll and carotenoid content might be a response to excessive production of ROS in chloroplasts (Liu et al., 2009).

Response of enzymatic antioxidant systems

High concentrations of nanomaterials promote the formation of ROS in living cells causing oxidative damages to cell structures and bio-molecules (Čapek and Roušar, 2021). As a consequence, cells have developed competent ROS scavenging systems comprising enzymatic and non-enzymatic antioxidants to balance the amount of ROS (Wang et al., 2019). In this section, the activities of a number of antioxidant enzymes after treatment of algae cells with different concentrations of MoO_3 NPs and $\{Mo_{36}\}$ NCs were evaluated.

SOD promotes superoxide breakdown into oxygen and H_2O_2, and therefore plays a critical role in battle of cells against oxidative stress. After treatment of cells with the increasing concentrations of NMs, the activity of SOD rose and subsequently fell (Fig. 7A, B). The maximum activity of SOD in the cells was observed after their exposure to 25 mgL^{-1} MoO_3 NPs and 50 mgL^{-1} $\{Mo_{36}\}$ NCs. Although in both cases, high concentrations of NMs led to harm to the enzymatic system, the damaging effect of MoO_3 NPs on

SOD was apparently higher than that of {Mo_{36}} NCs. Changes in the activity of SOD were shown also in some foregoing studies. A considerable upsurge of SOD activity in *Chlorella vulgaris* with the increasing concentration of ZnO nanoparticles was indicated (Feizi et al., 2022). By contrast, SOD activity has diminished in *Chlorella vulgaris* treated with CdSe NPs (Movafeghi et al., 2019). In another study, the increased and suppressed activity of SOD respectively at low and high concentrations of CeO_2 NPs was reported (Cui et al., 2014).

CAT is another essential antioxidant enzyme catalyzing the detoxification of hydrogen peroxide to molecular oxygen and water. We observed a concurrent increase in the activity of CAT with the ascending concentration of NMs. Comparing to NP treatments, {Mo_{36}} NCs caused a higher CAT activity. This higher enzymatic activity after exposure to {Mo_{36}} NCs was possibly attributable to the high solubility of {Mo_{36}} NCs and their fast entry into the cells (Fig. 7C, D). Enhancing the CAT activity was shown also in *Lemna minor* treated with CuO NPs (Song et al., 2016) and ZnSe NPs (Tarrahi et al., 2018). Also, activity of CAT in *Scenedesmus obliquus* has increased after exposure to SiO_2 and TiO_2 NPs (Liu et al., 2018). After treatment of *Nitzschia closterium* with increasing amounts of TiO_2 NPs the activity of CAT has first initiated, and then reduced (Xia et al., 2015). At low concentrations of NMs, antioxidant enzyme activity in algal cells rises to prevent ROS toxicity, however intense toxicity of NPs causes demolishing of enzymatic scavenging systems (Wang et al., 2019). Descent of CAT activity under harsh stress conditions is feasibly because of enzyme inactivation due to ROS accumulation and/or diminishing of enzyme synthesis (Verma and Dubey, 2003).

APX as the most abundant antioxidant enzyme reduces H_2O_2 to water and utilizes ascorbic acid as an electron donor. APX affinity to H_2O_2 is more than catalase and peroxidase, and thus it may act determinedly in the ROS management system (Caverzan et al., 2012). We distinguished enhancing APX activity after exposure of cells to the applied concentration of MoO_3 NPs and {Mo_{36}} NCs. Of note, such as changes in CAT and SOD activities, APX activity has also fell at the high concentrations of NMs, especially that of MoO_3 NPs. On the face of it, MoO_3 NPs showed higher toxic effect at the high concentrations on enzymatic antioxidant of cells (Fig. 7E, F). In accordance with our results, similar concentration-dependent increasing and decreasing trend in APX activity was also found in plants and algae under stress (Rai et al., 2013; Manaf et al., 2021).

Changes in the phenol and flavonoid content

Phenols and flavonoids are well-known non-enzymatic antioxidant compounds in plants and algae (Rezayian et al., 2019). Phenols have perfect structure for free radical scavenging and play crucial roles in chelating metal ions and removing ROS (Dumanović et al., 2021). As well, flavonoids are contributing in ROS modulation in cells experiencing biotic and abiotic stresses (Agati et al., 2020). Nonetheless, little data exists on the influence of NMs on the phenol and flavonoid content in microalgae. In the present study, the content of phenols in algal cells has heightened depending on the concentration of MoO_3 NPs (Fig. 8A). In comparison, treatment of cells with 25 mg L^{-1} of {Mo_{36}} NCs increased the level of phenols

and then higher NC concentrations led to a significant decline in phenol content (Fig. 8B). Flavonoid content has increased after exposure of cells to 25 and 50 mg L^{-1} of both nanomaterials and then went down at higher concentrations (Fig. 8C, D). Alteration of phenol and flavonoid contents was obviously correlated with cell defense machineries in reaction to the induced stress by nanomaterials. However, high concentrations of NMs caused seemingly a severe oxidative stress and reduced the content of phenolic and flavonoid compounds. Such disturbance in the non-enzymatic defense systems could result in the weakened antioxidant capacity of algal cells in response to high concentrations of NMs. Such alterations in the quantity of non-enzymatic compounds in *C. vulgaris* cells by MoO_3 NPs and $\{Mo_{36}\}$ NCs were in agreement with the preceding findings on the defense response of plant and algae cells to toxicity of NMs (Mahjouri et al. 2018; Movafeghi et al. 2019). In other words, the assortment of biological responses of living cells depends mainly on the type and concentration of NMs.

Conclusion

This study was conducted to investigate the induced cytotoxicity of MoO_3 NPs and $\{Mo_{36}\}$ NCs to C. *vulgaris* cells. Physicochemical characterization of the synthesized nanomaterials demonstrated their proper nano size and characteristics, which were suitable for entrance into the algal cells. The synthesized MoO_3 NPs and $\{Mo_{36}\}$ NCs were found to induce cytotoxicity in a hormetic dose-dependent manner. The toxicity was measurable through a decline in the cell growth and cell viability as well as changes in the morphology of the cells. Exposure to low concentrations of NMs heightened the content of photosynthetic pigments in algal cells, although the higher concentrations of NMs decrease their amounts. Algal cells struggled to handle the harmful effects of MoO_3 NPs and $\{Mo_{36}\}$ NCs by means of enzymatic and non-enzymatic antioxidant systems. At low concentrations of both NMs, antioxidant systems seemed to be capable to inhibit oxidative toxicity, nevertheless high concentrations of NPs led to defeating the antioxidative systems. Hereafter, complementary research is needed to explore the mechanisms of the toxicity of MoO_3 NPs and $\{Mo_{36}\}$ NCs on the algal cells, and also to determine the resistance strategies of the exposed cells to manage the stress-induced condition.

Declarations

Ethical approval Not applicable

Consent to participate Not applicable

Consent for publication Not applicable

Authors' contributions HA Kalehjahi, M Kosari-Nasab, and A Movafeghi planned the research. HA Kalehjahi conducted the experiments. M. Amini contributed to carry out the synthesis and characterization of nanomaterials. The first draft of the manuscript was written by HA Kalehjahi and A Movafeghi and all authors commented on preceding versions of the manuscript. All authors read and approved the final manuscript.

Funding This research received no funds during the preparation of this manuscript.

Competing interests The authors declare that they have no competing interests.

Availability of data and materials All data generated or analyzed during this work are included in the manuscript file.

References

1. Agati G, Brunetti C, Fini A, Gori A, Guidi L, Landi M, Sebastiani F, Tattini M (2020) Are flavonoids effective antioxidants in plants? Twenty years of our investigation. Antioxidants 9:1098. https://doi.org/10.3390/antiox9111098
2. Alghamdi SB (2020) MoO_3 nano-bricks as novel antimicrobial agents. Eur J Biol Biotechnol 1:1–4. https://doi.org/10.24018/ejbio.2020.1.6.134
3. Amini M, Naslhajian H, Farnia SMF, Hołyńska M (2015) Selective oxidation of sulfides catalyzed by the nanocluster polyoxomolybdate $(NH_4)_{12}[Mo_{36}(NO)_4O_{108}(H_2O)_{16}]$. Eur J Inorg Chem 23:3873–3878. https://doi.org/10.1002/ejic.201500528
4. Asghari S, Rajabi F, Tarrahi R, Salehi-Lisar SY, Asnaashari S, Omidi Y (2020) Potential of the green microalga *Chlorella vulgaris* to fight against fluorene contamination: evaluation of antioxidant systems and identification of intermediate biodegradation. J of Appl Phycol 32:411–419. https://doi.org/10.1007/s10811-019-01921-7
5. Bhuvaneshwari M, Iswarya V, Archanaa S, Madhu G, Kumar GS, Nagarajan R, Chandrasekaran N, Mukherjee A (2015) Cytotoxicity of ZnO NPs towards fresh water algae *Scenedesmus obliquus* at low exposure concentrations in UV-C, visible and dark conditions. Aquat Toxicol 162:29–38. https://doi.org/10.1016/j.aquatox.2015.03.004
6. Bradford MM (1976) A rapid and sensitive method for the quantitation of microgram quantities of protein utilizing the principle of protein-dye binding. Anal Biochem 72:248–254. https://doi.org/10.1016/0003-2697(76)90527-3
7. Čapek J, Roušar T (2021) Detection of oxidative stress induced by nanomaterials in cells—The roles of reactive oxygen species and glutathione. Molecules 26:4710. https://doi.org/10.3390/molecules26164710
8. Caverzan A, Passaia G, Rosa SB, Ribeiro CW, Lazzarotto F, Margis-Pinheiro M (2012) Plant responses to stresses: Role of ascorbate peroxidase in the antioxidant protection. Genet Mol Biol 35(4 Suppl):1011–1019. https://doi.org/10.1590/s1415-47572012000600016.)
9. Chance B, Maehly AC (1955) Assay of catalases and peroxidases. Meth Enzymol 2:764–775. http://dx.doi.org/10.1016/S0076-6879(55)02300-8
10. Chang C-C, Yang M-H, Wen H-M, Chern J-C (2002) Estimation of total flavonoid content in propolis by two complementary colorimetric methods. J Food Drug Anal 10:178–182. https://doi.org/10.38212/2224-6614.2748

11. Cheng J, Qiu H, Chang Z, Jiang Z, Yin W (2016) The effect of cadmium on the growth and antioxidant response for freshwater algae *Chlorella vulgaris*. Springerplus 5:1290. https://doi.org/10.1186/s40064-016-2963-1
12. Cheng L, Shao M, Wang X, Hu H (2009) Single-crystalline molybdenum trioxide nanoribbons: photocatalytic, photoconductive, and electrochemical properties. Chem Eur J 15:2310–2316. https://doi.org/10.1002/chem.200802182
13. Cui D, Zhang P, Ma Y, He X, Li Y, Zhang J, Zhao Y, Zhang Z (2014) Effect of cerium oxide nanoparticles on asparagus lettuce cultured in an agar medium. Environ Sci Nano 1:459–465. https://doi.org/10.1039/C4EN00025K
14. Dumanović J, Nepovimova E, Natić M, Kuča K, Jaćević V (2021) The significance of reactive oxygen species and antioxidant defense system in plants: a concise overview. Front Plant Sci 6:552969. https://doi.org/10.3389/fpls.2020.552969
15. Fazelian N, Movafeghi A, Yousefzadi M, Rahimzadeh M (2019) Cytotoxic impacts of CuO nanoparticles on the marine microalga *Nannochloropsis oculata*. Environ Sci Pollut Res 26:17499–17511. https://doi.org/10.1007/s11356-019-05130-0
16. Feizi S, Kosari-Nasab M, Divband B, Mahjouri S, Movafeghi A (2022) Comparison of the toxicity of pure and samarium-doped zinc oxide nanoparticles to the green microalga *Chlorella vulgaris*. Environ Sci Pollut Res 29:32002–32015. https://doi.org/10.1007/s11356-022-18539-x
17. Forloni G (2012) Responsible nanotechnology development. J Nanopart Res 14:1–17. https://doi.org/10.1007/ s11051-012-1007-1
18. Giese B, Klaessig F, Park B, Kaegi R, Steinfeldt M, Wigger H, von Gleich A, Gottschalk F (2018) Risks, release and concentrations of engineered nanomaterial in the environment. Sci Rep 8:1565. https://doi.org/10.1038/s41598-018-19275-4
19. Jalilian F, Yadollahi B, Farsani MR, Tangestaninejad S, Rudbari HA, Habibi R (2015) New perspective to Keplerate polyoxomolybdates: Green oxidation of sulfides with hydrogen peroxide in water. Catal Commun 66:107–110. https://doi.org/10.1016/j.catcom.2015.03.032
20. Ji J, Long Z, Lin D (2011) Toxicity of oxide nanoparticles to the green algae *Chlorella* sp. Chem Eng J 170:525–530. https://doi.org/10.1016/j.cej.2010.11.026
21. Juárez-Maldonado A, Tortella G, Rubilar O, Fincheira P, Benavides-Mendoza A (2021) Biostimulation and toxicity: The magnitude of the impact of nanomaterials in microorganisms and plants. J Adv Res 31:113–126. https://doi.org/10.1016/j.jare.2020.12.011
22. Kalhor AX, Movafeghi A, Mohammadi-Nassab AD, Abedi E, Bahrami A (2017) Potential of the green alga *Chlorella vulgaris* for biodegradation of crude oil hydrocarbons. Mar Pollut Bull 123:286–290. https//doi.org/10.1016/j.marpolbul.2017.08.045
23. Khoshnamvand M, Ashtiani S, Chen Y, Liu J (2020) Impacts of organic matter on the toxicity of biosynthesized silver nanoparticles to green microalgae *Chlorella vulgaris*. Environ Res 185:109433. https//doi.org/10.1016/j.envres.2020.109433

24. Liu H, Weisman D, Ye YB, Cui B, Huang YH, Colón-Carmona A, Wang ZH (2009) An oxidative stress response to polycyclic aromatic hydrocarbon exposure is rapid and complex in *Arabidopsis thaliana*. Plant Sci 176:375–382. https://doi.org/10.1016/j.plantsci.2008.12.002
25. Liu Y, Wang S, Wang Z, Ye N, Fang H, Wang D (2018) TiO_2, SiO_2 and ZrO_2 nanoparticles synergistically provoke cellular oxidative damage in freshwater microalgae. Nanomaterials 8:95. https://doi.org/10.3390/nano8020095
26. Lütz-Meindl U, Lütz C (2006) Analysis of element accumulation in cell wall attached and intracellular particles of snow algae by EELS and ESI. Micron 37:452–458. https://doi.org/10.1016/j.micron.2005.11.004
27. Malakar A, Kanel SR, Ray C, Snow DD, Nadagouda MN (2021) Nanomaterials in the environment, human exposure pathway, and health effects: A review. Sci Total Environ 759:143470. https://doi.org/10.1016/j.scitotenv.2020.143470
28. Manaf A, Wang X, Tariq F, Jhanzab HM, Bibi Y, Sher A, Razzaq A, Fiaz S, Tanveer SK, Qayyum A (2021) Antioxidant enzyme activities correlated with growth parameters of wheat sprayed with silver and gold nanoparticle suspensions. Agronomy 11:1494. https://doi.org/10.3390/agronomy11081494
29. Meda A, Lamien CE, Romito M, Millogo J, Nacoulma OG (2005) Determination of the total phenolic, flavonoid and proline contents in Burkina Fasan honey, as well as their radical scavenging activity. Food Chem 91:571–577. https://doi.org/10.1016/j.foodchem.2004.10.006
30. Mendel RR, Bittner F (2006) Cell biology of molybdenum. Biochim Biophys Acta 1763:621–635. https://doi.org/10.1016/j.bbamcr.2006.03.013
31. Metzler DM, Erdem A, Tseng YH, Huang CP (2012) Responses of algal cells to engineered nanoparticles measured as algal cell population, chlorophyll a, and lipid peroxidation: effect of particle size and type. J Nanotechnol 237284:1–12. https://doi.org/10.1155/2012/237284
32. Monteiro CM, Castro PM, Malcata FX (2012) Metal uptake by microalgae: underlying mechanisms and practical applications. Biotechnol Prog 28:299–311. https://doi.org/10.1002/btpr.1504
33. Movafeghi A, Khataee A, Abedi M, Tarrahi R, Dadpour M, Vafaei F (2018) Effects of TiO_2 nanoparticles on the aquatic plant *Spirodela polyrrhiza*: Evaluation of growth parameters, pigment contents and antioxidant enzyme activities. J Environ Sci 64:130–138. https://doi.org/10.1016/j.jes.2016.12.020
34. Movafeghi A, Khataee A, Rezaee A, Kosari-Nasab M, Tarrahi R (2019) Toxicity of cadmium selenide nanoparticles on the green microalga *Chlorella vulgaris*: inducing antioxidative defense response. Environ Sci Pollut Res 26:36380–36387. https://doi.org/10.1007/s11356-019-06675-w
35. Nakano Y, Asada K (1981) Hydrogen peroxide is scavenged by ascorbate-specific peroxidase in spinach chloroplasts. Plant Cell Physiol 22:867–880. https://doi.org/10.1093/oxfordjournals.pcp.a076232
36. Navarro E, Baun A, Behra R, Hartmann NB, Filser J, Miao AJ, Quigg A, Santschi PH, Sigg L (2008) Environmental behavior and ecotoxicity of engineered nanoparticles to algae, plants, and fungi.

Ecotoxicology 17:372–386. https://doi.org/10.1007/s10646-008-0214-0

37. Nazari F, Movafeghi A, Jafarirad S, Kosari-Nasab M, Divband B (2018) Synthesis of reduced graphene oxide-silver nanocomposites and assessing their toxicity on the green microalga *Chlorella vulgaris*. Bionanoscience 8:997–1007. https://doi.org/10.1007/s12668-018-0561-0
38. Pereira MM, Mouton L, Yéprémian C, Couté A, Lo J, Marconcini JM, Ladeira LO, Raposo NR, Brandão HM, Brayner R (2014) Ecotoxicological effects of carbon nanotubes and cellulose nanofibers in *Chlorella vulgaris*. J Nanobiotechnol 12:1–13. https://doi.org/10.1186/1477-3155-12-15
39. Rai UN, Singh NK, Upadhyay AK, Verma S (2013) Chromate tolerance and accumulation in *Chlorella vulgaris* L.: Role of antioxidant enzymes and biochemical changes in detoxification of metals. Bioresour Technol 136:604–609. https://doi.org/10.1016/j.biortech.2013.03.043
40. Rezayian M, Niknam V, Ebrahimzadeh H (2019) Oxidative damage and antioxidative system in algae. Toxicol Rep 24:1309–1313. https://. doi
41. Saxena P, Saharan V, Baroliya PK, Gour VS, Rai MK (2021) Mechanism of nanotoxicity in *Chlorella vulgaris* exposed to zinc and iron oxide. Toxicol Rep 8:724–731. https://doi.org/10.1016/j.toxrep.2021.03.023
42. Shafaei S, Dörrstein J, Guggenbichler JP, Zollfrank C (2017) Cellulose acetate-based composites with antimicrobial properties from embedded molybdenum trioxide particles. Lett Appl Microbiol 64:43–50. https://doi.org/10.1111/lam.12670
43. Song G, Hou W, Gao Y, Wang Y, Lin L, Zhang Z, Niu Q, Ma R, Mu L, Wang H (2016) Effects of CuO nanoparticles on *Lemna minor*. Bot Stud 57:1–8. https://doi.org/10.1186/s40529-016-0118-x
44. Stamate AE, Pavel OD, Zavoianu R, Marcu IC (2020) Highlights on the catalytic properties of polyoxometalate-intercalated layered double hydroxides: A review. Catalysts 10:57. https://doi.org/10.3390/catal10010057
45. Suhendra E, Chang C-H, Hou W-C, Hsieh Y-C (2020) Review on the environmental fate models for predicting the distribution of engineered nanomaterials in surface waters. Int J Mol Sci 21:4554. https://doi.org/10.3390/ijms21124554.)
46. Suman T, Rajasree SR, Kirubagaran R (2015) Evaluation of zinc oxide nanoparticles toxicity on marine algae *Chlorella vulgaris* through flow cytometric, cytotoxicity and oxidative stress analysis. Ecotoxicol Environ Saf 113:23–30. https://doi.org/10.1016/j.ecoenv.2014.11.015
47. Taghizadeh SM, Berenjian A, Chew KW, Show PL, Zaid HFM, Ramezani H, Ghasemi Y, Raee MJ, Ebrahiminezhad A (2020) Impact of magnetic immobilization on the cell physiology of green unicellular algae *Chlorella vulgaris*. Bioengineered 11:141–153. https://doi.org/10.1080/21655979.2020.1718477
48. Tarrahi R, Khataee A, Movafeghi A, Rezanejad F (2018) Toxicity of ZnSe nanoparticles to *Lemna minor*: Evaluation of biological responses. J Environm Manage 226:298–307. https://doi.org/10.1016/j.jenvman.2018.08.036
49. Verma S, Dubey RS (2003) Lead toxicity induces lipid peroxidation and alters the activities of antioxidant enzymes in growing rice plants. Plant Sci 164:645–655. https://doi.org/10.1016/S0168-

9452(03)00022-0

50. Wang F, Guan W, Xu L, Ding Z, Ma H, Ma A, Terry N (2019) Effects of nanoparticles on algae: Adsorption, distribution, ecotoxicity and fate. Appl Sci 9:1534. https://doi.org/10.3390/app9081534
51. Wang D, Lin Z, Wang T, Yao Z, Qin M, Zheng S, Lu W (2016) Where does the toxicity of metal oxide nanoparticles come from: The nanoparticles, the ions, or a combination of both? J Hazard Mater 5:328–334. doi: 10.1016/j.jhazmat.2016.01.066
52. Wang F, Liu T, Guan W, Xu L, Huo S, Ma A, Zhuang G, Terry N (2021) Development of a strategy for enhancing the biomass growth and lipid accumulation of *Chlorella* sp. UJ-3 using magnetic Fe_3O_4 nanoparticles. Nanomaterials 11:2802. https://doi.org/10.3390/nano11112802.)
53. Wellburn AR (1994) The spectral determination of chlorophylls a and b, as well as total carotenoids, using various solvents with spectrophotometers of different resolution. J Plant Physiol 144:307–313. https://doi.org/10.1016/S0176-1617(11)81192-2
54. Winterbourn CC, McGrath BM, Carrell RW (1976) Reactions involving superoxide and normal and unstable haemoglobins. Biochem J 155:493–502. https://doi.org/10.1042/bj1550493
55. Xia B, Chen B, Sun X, Qu K, Ma F, Du M (2015) Interaction of TiO_2 nanoparticles with the marine microalga *Nitzschia closterium*: growth inhibition, oxidative stress and internalization. Sci Total Environ 508:525–533. https://doi.org/10.1016/j.scitotenv.2014.11.066
56. Xiaoxiao C, Xing Z, Rui L, Hanchao Y, Zhisong L, Xu Y (2012) Photosynthetic toxicity and oxidative damage induced by nano-Fe_3O_4 on *Chlorella vulgaris* in aquatic environment. Open J Ecol 2:21–28. https://doi.org/10.4236/oje.2012.21003
57. Xue S, Cao S, Huang Z, Yang D, Zhang G (2021) Improving gas-sensing performance based on MOS nanomaterials: A review. Materials 14:4263. https://doi.org/10.3390/ma14154263
58. Zhao J, Lin M, Wang Z, Cao X, Xing B (2021) Engineered nanomaterials in the environment: Are they safe? Crit Rev Environ Sci Technol 51:1443–1478. https://doi.org/10.1080/10643389.2020.1764279

Figures

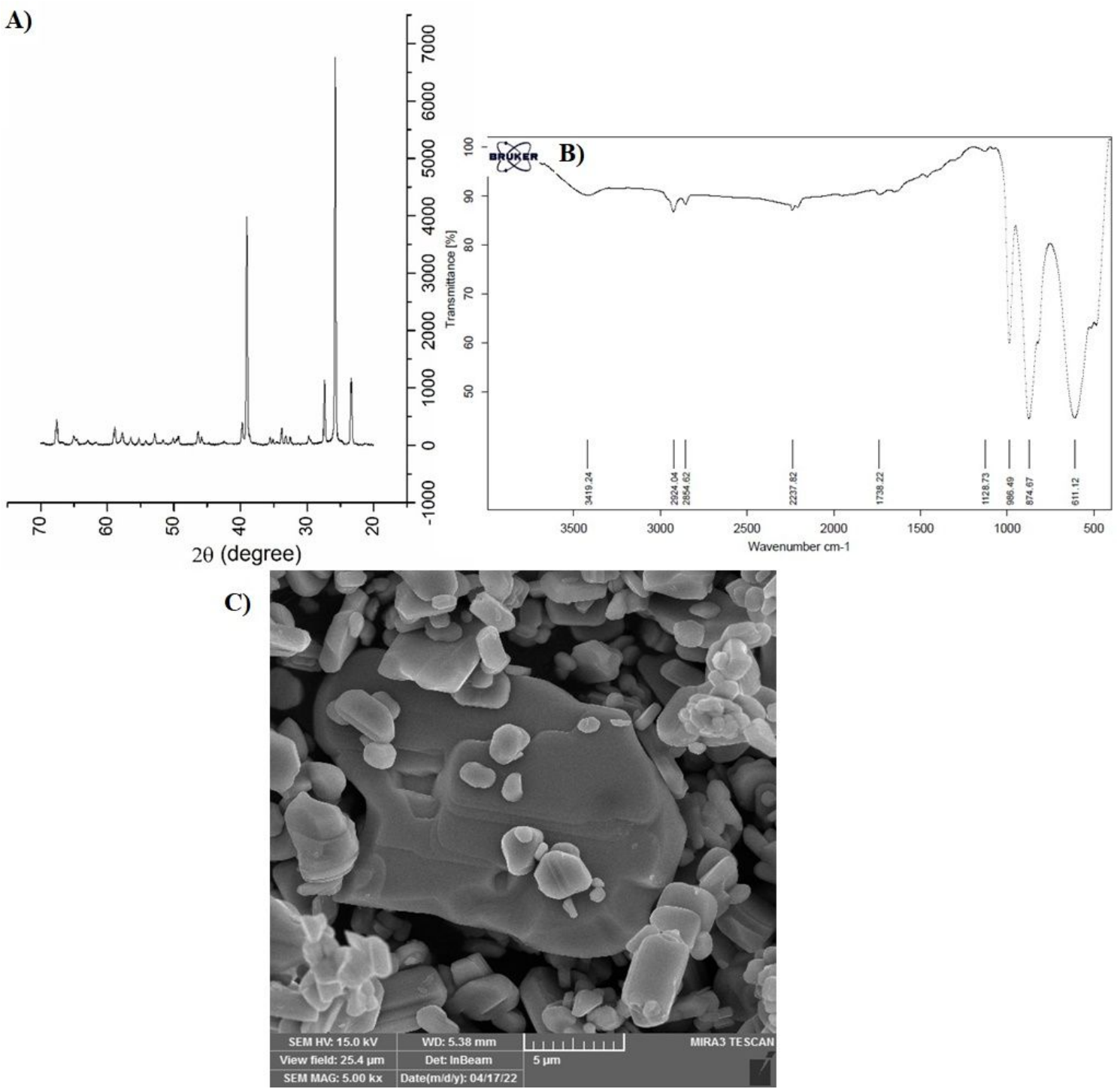

Figure 1

Characteristics of the synthesized MoO_3 NPs; XRD pattern (A), FTIR spectrum (B), and SEM image (C).

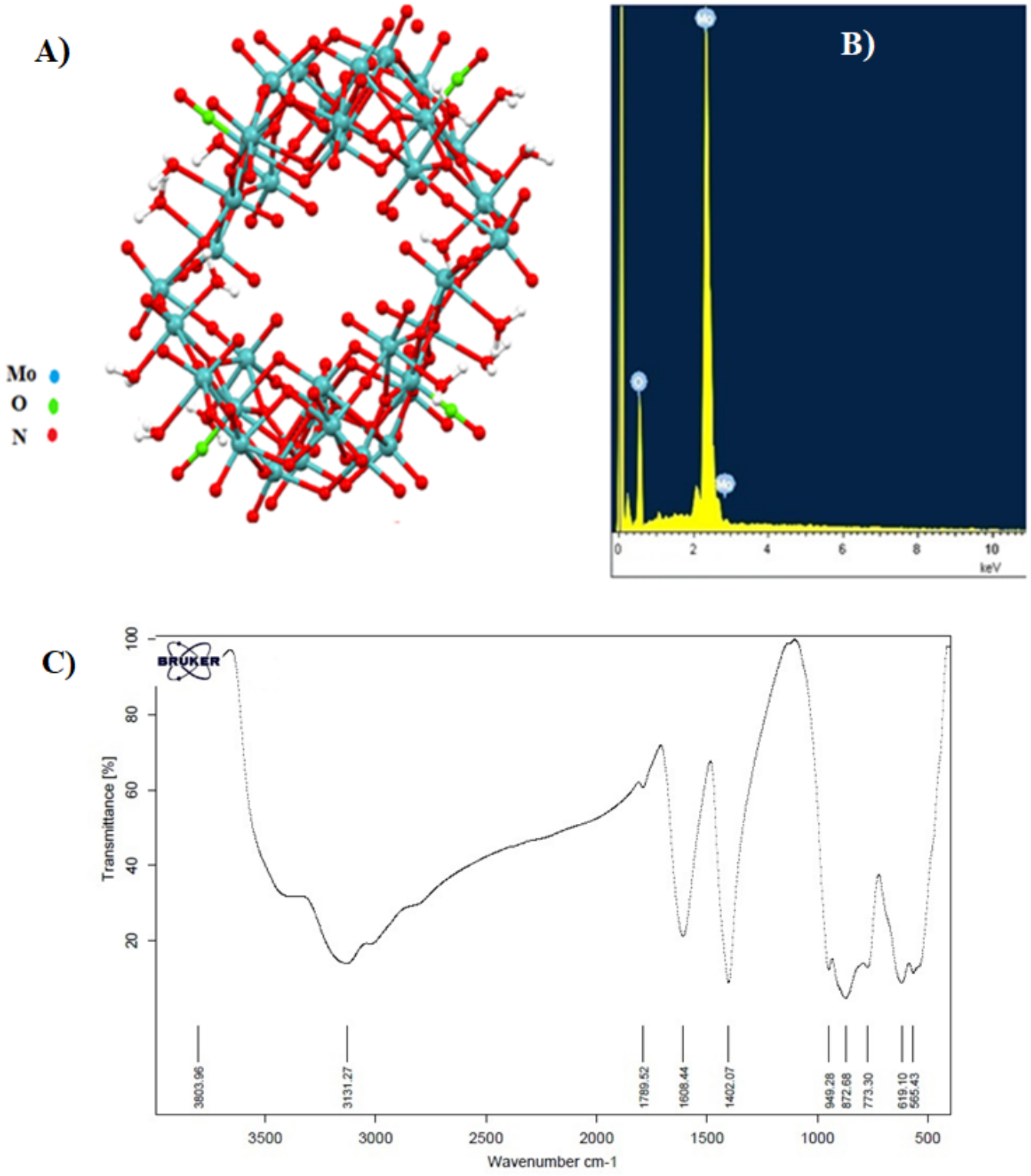

Figure 2

Features of the synthesized {Mo_{36}} NCs. View of the {Mo_{36}} NCs with labeling of the atoms (A), EDX analysis (B), and FTIR spectrum (C).

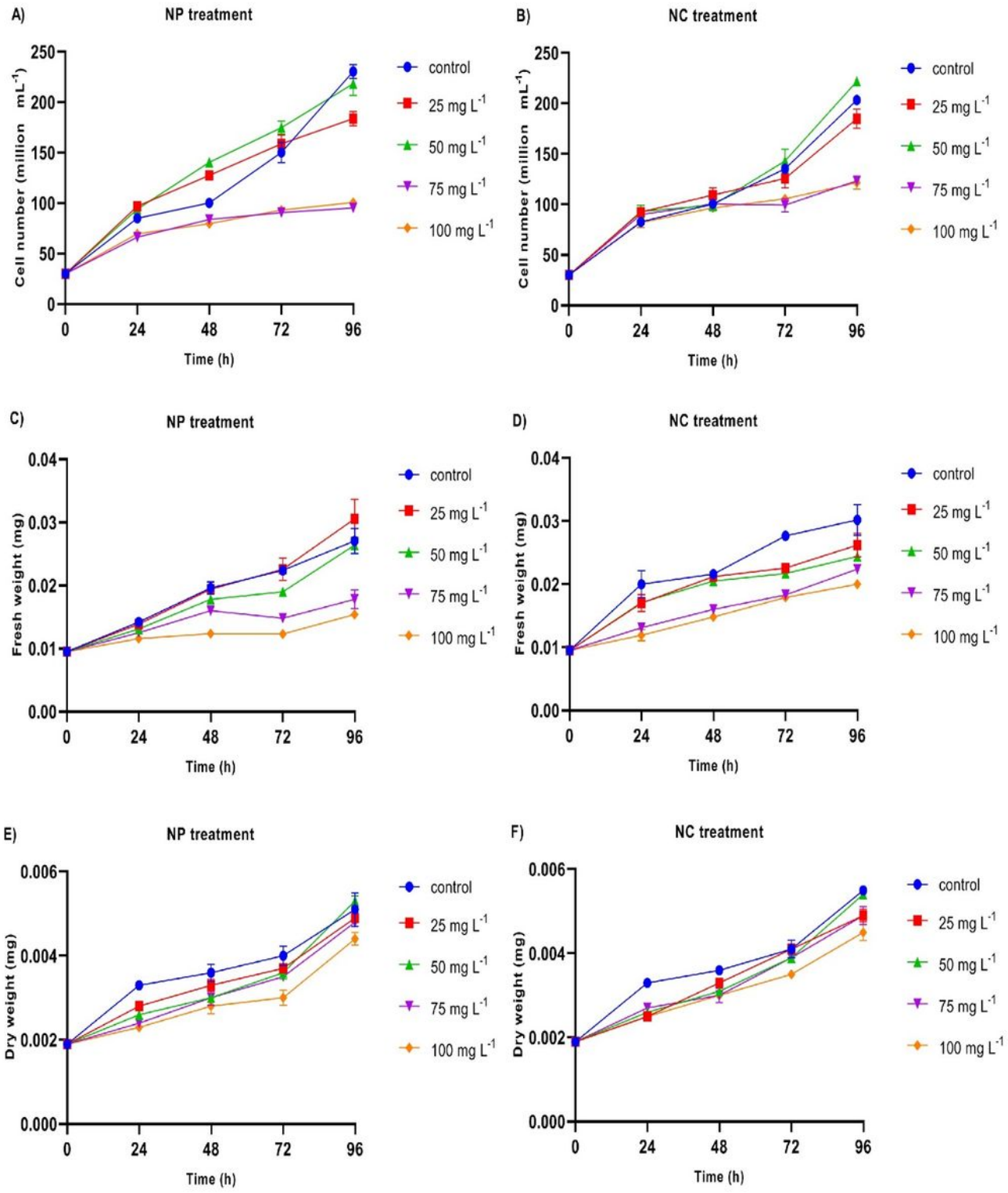

Figure 3

The concentration-dependent effects of MoO_3 NPs and $\{Mo_{36}\}$ NCs on cell number (A, B), fresh weight (C, D) and dry weight (E, F) of *C. vulgaris* Different letters indicate significant differences according to Duncan's Test at $P < 0.05$. The data are indicated as means ± SE (n=3).

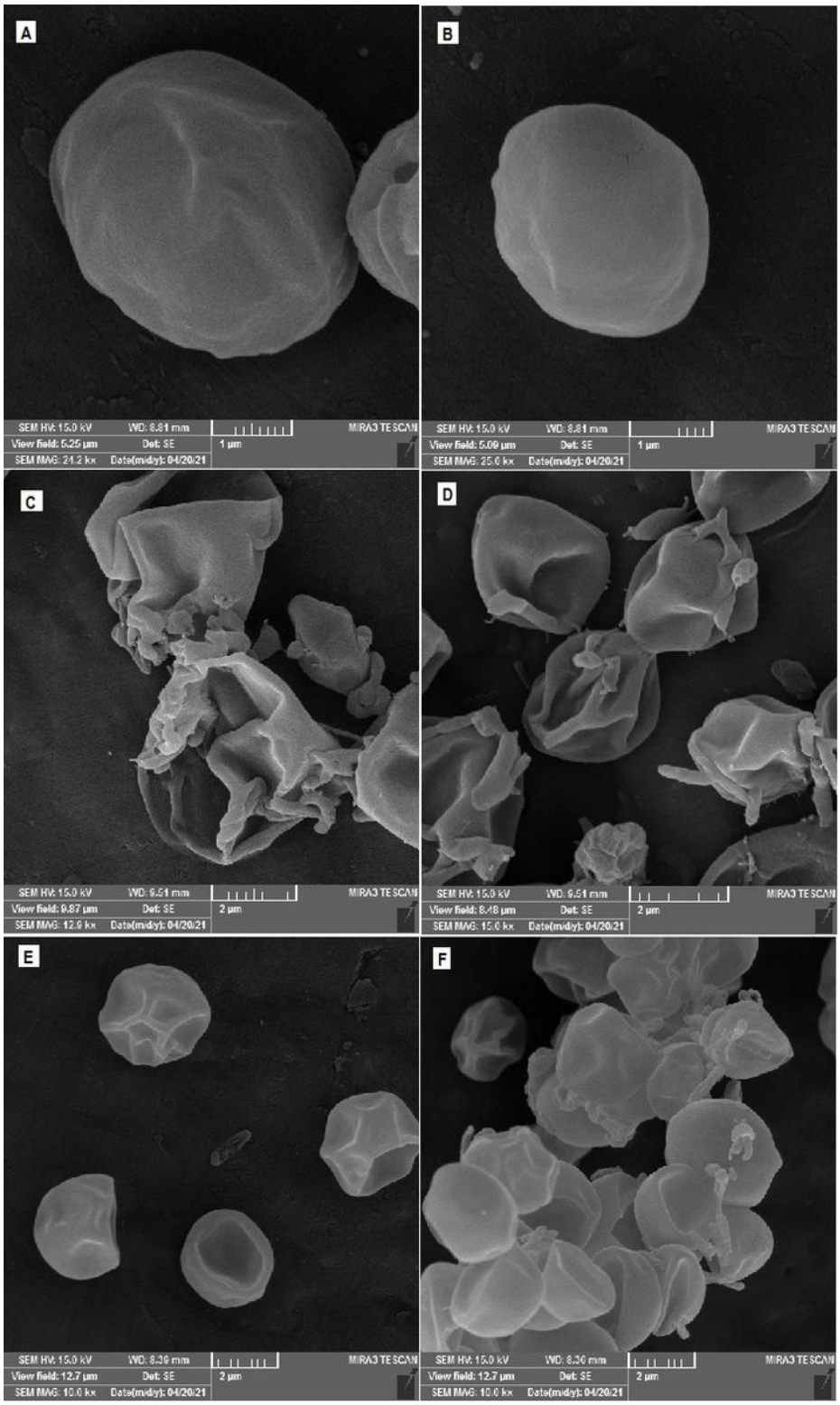

Figure 4

Morphological changes of *C. vulgaris* cells after exposure to MoO_3 NPs and $\{Mo_{36}\}$ NCs. SEM images of control samples (A, B). Algal cells after treatment with 100 mg L^{-1} of MoO_3 NPs (C, D) and $\{Mo_{36}\}$ NCs (E, F).

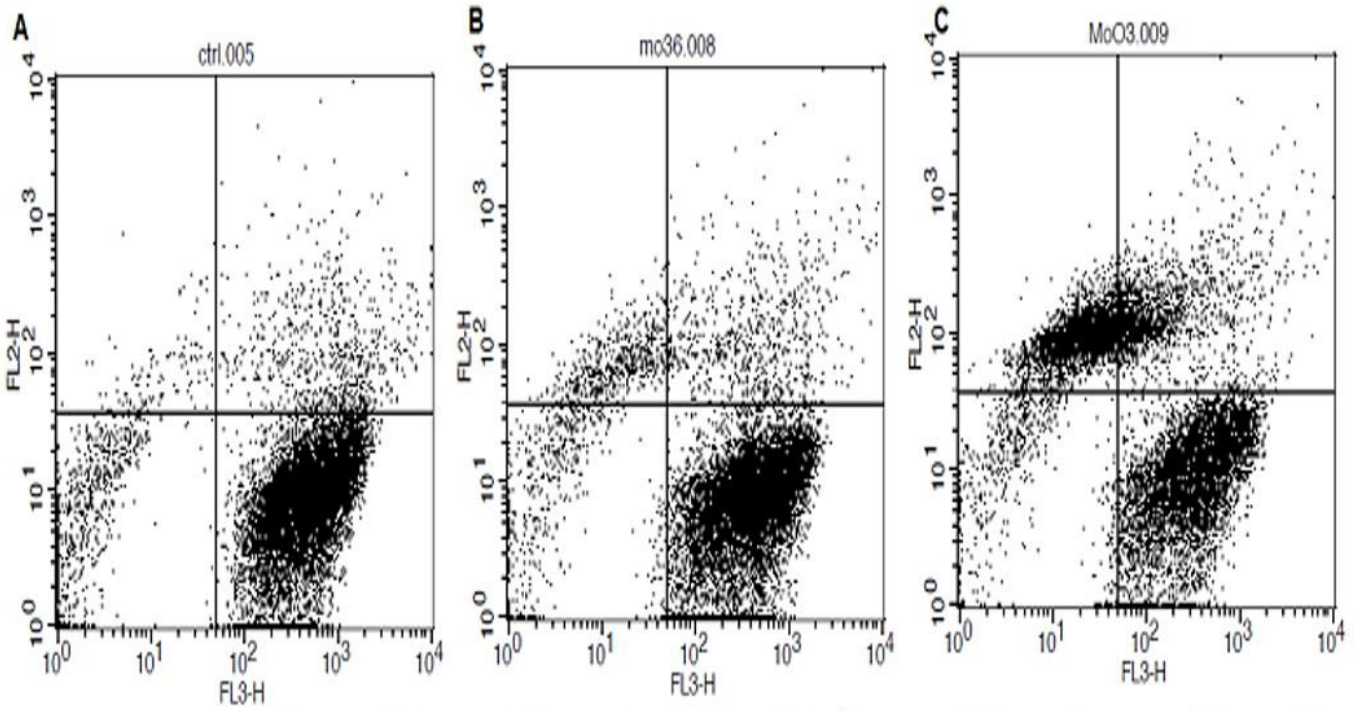

Quad	Events	% Gated	% Total	X Mean	Y Mean
UL	121	1.21	1.21	16.79	94.54
UR	723	7.23	7.23	1399.32	192.48
LL	682	6.82	6.82	3.26	10.01
LR	8474	84.74	84.74	572.93	9.44

Quad	Events	% Gated	% Total	X Mean	Y Mean
UL	552	5.52	5.52	18.60	81.20
UR	688	6.88	6.88	885.90	233.57
LL	501	5.01	5.01	7.40	12.31
LR	8259	82.59	82.59	506.09	8.51

Quad	Events	% Gated	% Total	X Mean	Y Mean
UL	2628	26.28	26.28	23.36	95.93
UR	1678	16.78	16.78	368.22	197.33
LL	521	5.21	5.21	10.01	13.03
LR	5173	51.73	51.73	427.77	10.61

Figure 5

Flow cytometry analysis. Control sample showed nearly 92% of cell viability (A). After treatment of *C. vulgaris* with 100 mg L^{-1} $\{Mo_{36}\}$ NCs for 96 h viability of the cells has declined to ~ 87% (B). (C) Cell viability of *C. vulgaris* treated with 100 mg L^{-1} MoO_3 NPs for 4 days has lessened to ~ 57 %.

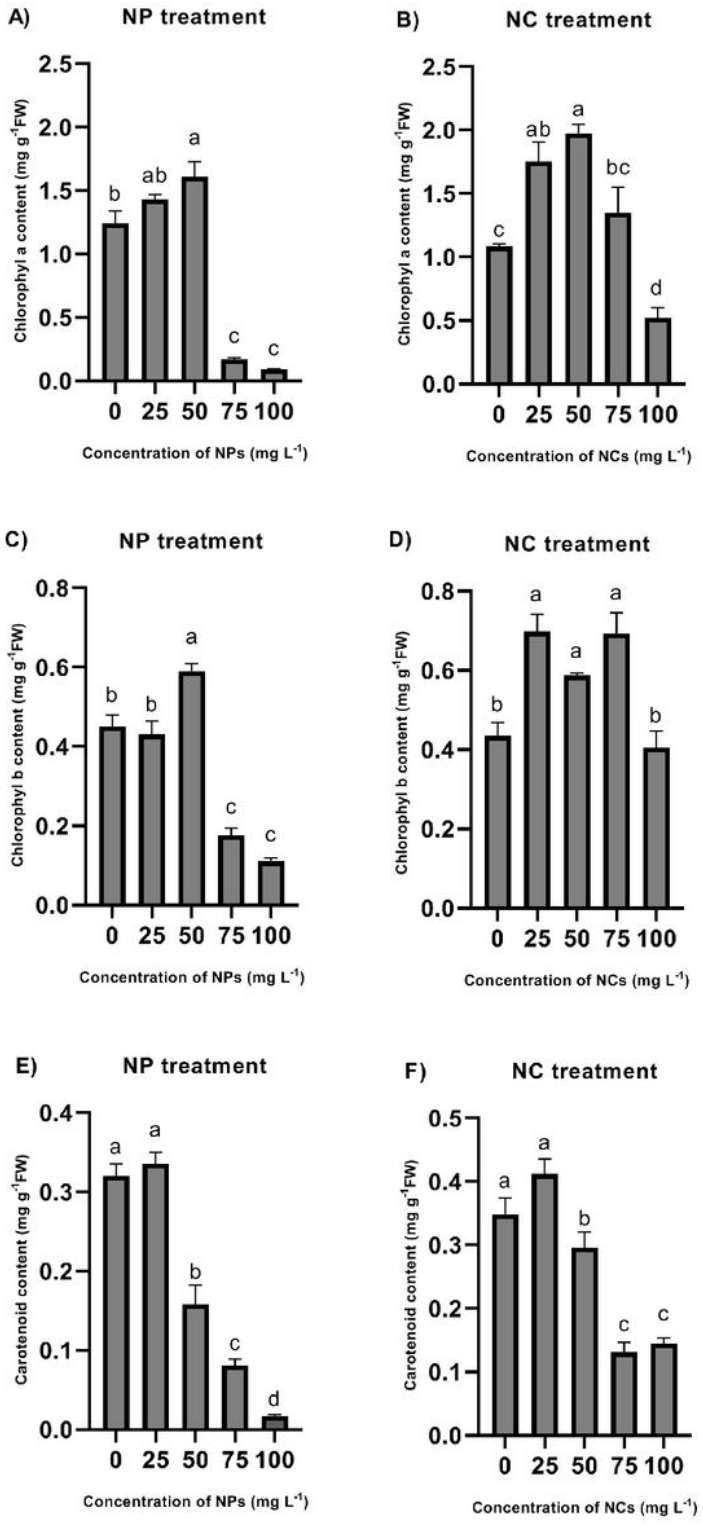

Figure 6

Effects of different concentrations of MoO_3 NPs (A, C and E) and {Mo_{36}} NCs (B, D and F) on photosynthetic pigment contents in *C. vulgaris* after 96 h of exposure. Different letters show significant differences according to Duncan's test at $P < 0.05$. The results are indicated as means ± SE (n=3).

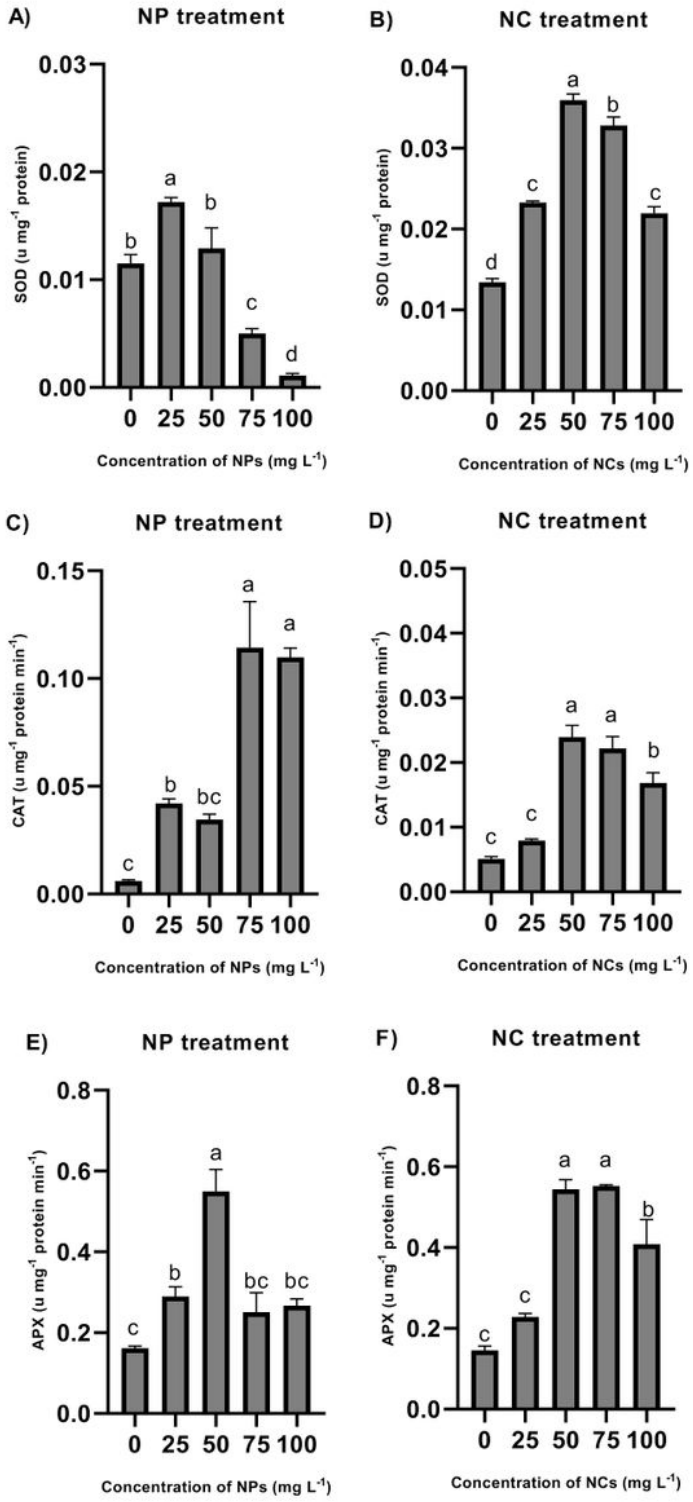

Figure 7

Activity of SOD (A, B), CAT (C, D) and APX (E, F) in algal cells after a 96-houre-exposure to MoO_3 NPs and and $\{Mo_{36}\}$ NCs. Different letters indicate significant differences according to Duncan's test at $P < 0.05$. The results are indicated as means ± SE (n=3).

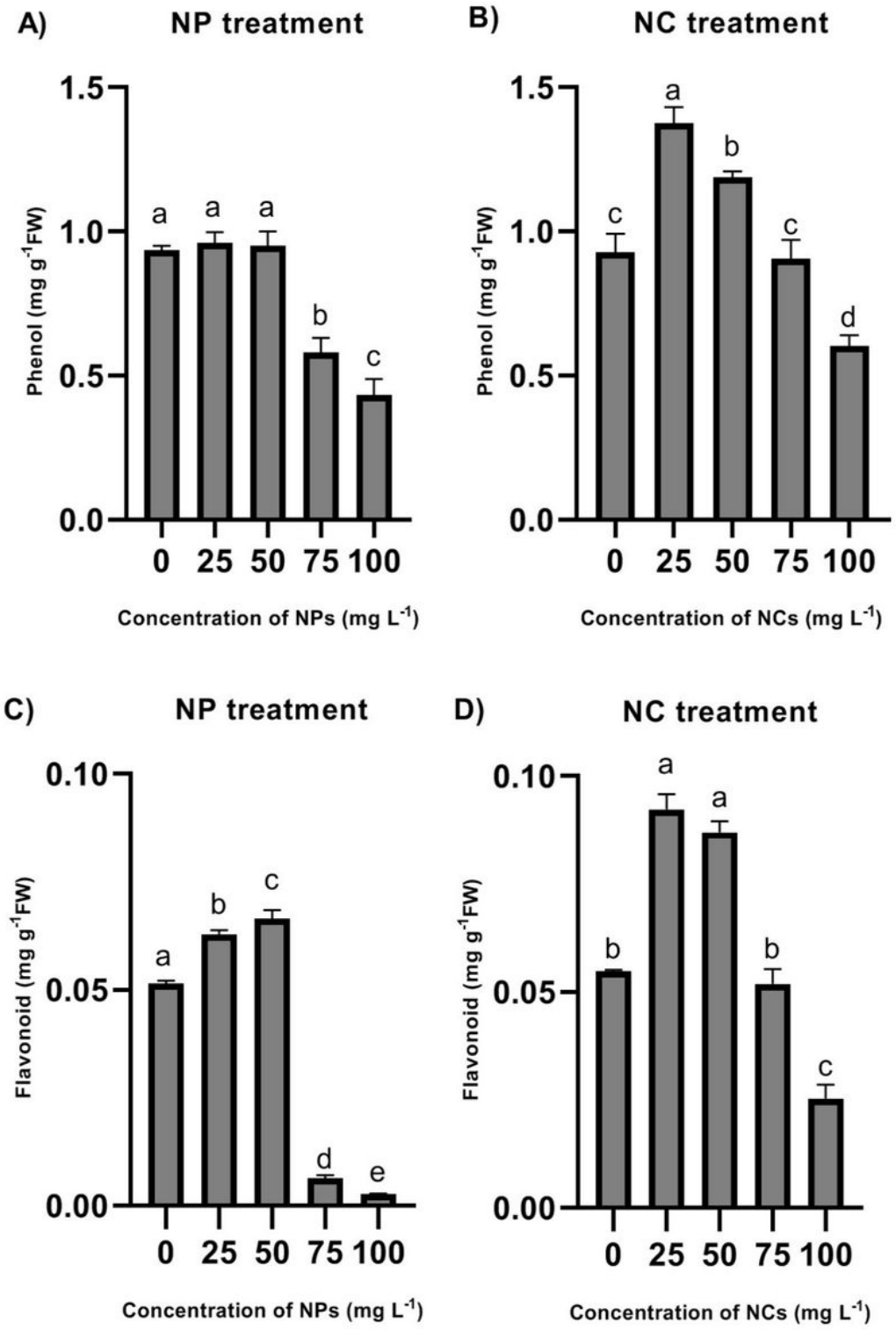

Figure 8

Influence of different concentrations of MoO_3 NPs and {Mo_{36}} NCs on phenol and (A, B) and flavonoid content (C, D) of *C. vulgaris* after 96 h of exposure. Different letters indicate significant differences according to Duncan's test at $P < 0.05$. The results are indicated as means ± SE (n=3).